JOURNAL OF CATALYSIS 107, 161–172 (1987)

Study on Reaction Rates for Methanol Synthesis from Carbon Monoxide, Carbon Dioxide, and Hydrogen

MAKOTO TAKAGAWA AND MINORU OHSUGI

Niigata Research Laboratories, Mitsubishi Gas Chemical Company Incorporated,
182 Tayuhama-shinwari, Niigata, 950-31 Japan

Received October 31, 1985; revised April 8, 1987

The reaction rates for methanol synthesis from carbon monoxide, carbon dioxide, and hydrogen over a copper–zinc-based catalyst were measured under the following conditions: temperature, 210–300°C; pressure, 4–10 MPa, feed gas compositions H_2/CO 2.7–720, H_2/CO_2, 4.3–120, CO_2/CO, 0.05–180 (in moles). It was concluded that direct methanol production from CO_2 takes place under the above conditions in addition to the two well-known reactions, methanol synthesis from CO and CO formation from CO_2. Empirical rate equations for the three reactions were derived. From the viewpoint of reaction rates, the effect of each component, especially that of CO_2, was discussed. © 1987 Academic Press, Inc.

INTRODUCTION

Currently in the industrial methanol synthesis, Cu-Zn-based catalysts are widely used, and methanol is produced from the mixture of CO, CO_2, and H_2. It has been believed that two reactions [R-1] and [R-2] principally contribute to the industrial methanol synthesis (*1, 2*). This means that methanol is produced from CO, and CO_2 is just a source of CO.

$$CO + 2H_2 \rightleftarrows CH_3OH \qquad [R-1]$$

$$CO_2 + H_2 \rightleftarrows CO + H_2O \qquad [R-2]$$

Recently, other aspects of the contribution of CO_2 in the methanol synthesis have been reported. Some authors reported that methanol is produced directly from CO_2 through reaction [R-3] (*3–8*),

$$CO_2 + 3H_2 \rightleftarrows CH_3OH + H_2O, \qquad [R-3]$$

and the others concluded that CO_2 makes the catalyst surface active (*9*).

As for the former, the experimental conditions were different from the actual ones, except those of Rozovskii (*5*). In some studies, reaction pressures were lower (1 atm (= 101.3 kPa)) than those of the actual conditions, though $CO–CO_2–H_2$ systems were used as feed gases (*7, 8*). In the others, $CO_2–H_2$ feed gas systems were used under pressures of the actual conditions (*3, 4, 6*); that is, the contribution of CO was neglected. Rozovskii *et al.* (*5*) chose the conditions similar to the actual ones; however, they neglected [R-1] and concluded that methanol is produced from CO_2 only and CO is just a source of CO_2.

The activating effect of CO_2 was pointed out by Klier *et al.* (*9*). They reported that the active center of the catalyst undergoes a redox reaction with the gas-phase CO and CO_2. They also concluded that at low concentrations CO_2 acts as a promoter and at high concentrations as a retardant; as a result, an optimum value in CO_2/CO ratios exists for the rate of methanol synthesis. On the other hand, Liu *et al.* (*10*) reported that the initial rate of methanol production becomes larger monotonously with an increase in CO_2/CO ratios. Unfortunately, the degree of contribution of CO_2 to the actual methanol synthesis has not been confirmed clearly, so far.

Also, many kinetic studies have been reported on methanol synthesis (*2, 9, 11–14*). However, most of them were based on the experiments without CO_2. Klier *et al.* (*9*) and Villa *et al.* (*2*) reported the kinetic

0021-9517/87 $3.00

studies with CO–CO_2–H_2 feed gas systems. However, the former study was focused on the methanol synthesis from CO and H_2, and in the latter [R-3] was neglected. Van Herwijnen and DeJong (*15*) reported a kinetic study on [R-2], but it was carried out under low pressures (1–6 atm) in the absence of methanol formation. Consequently, a plausible kinetic study for the actual methanol synthesis in CO–CO_2–H_2 systems has not been reported, so far. In the present study, the authors studied the reaction mechanism in the actual methanol synthesis and tried to estimate the contribution of the respective reactions through a kinetic study.

EXPERIMENTAL

Reaction rate measurements were carried out with a conventional flow reactor equipped with a fixed catalyst bed. Figure 1 shows the flow diagram of the apparatus. The reactor R is a SUS304 tube (inner diameter, 6 mm; outer diameter, 32 mm) equipped with Nichrome wire on the outer wall. In all experiments, the temperature gradient along the catalyst bed (height, 14 mm) was less than 2.5°C.

Mixtures of CO, CO_2, H_2, CH_4, and N_2 were used as feed gases. They were prepared in a gas holder G. The feed gas was introduced to a compressor C, compressed, led to a purifying column PC1, and stored in an accumulator AC1. The gas with a specific composition ($CO/CO_2/H_2/CH_4 + N_2$ = 23/6.5/69.5/1 in mol%) was stored in another accumulator AC2 for reduction of the catalyst and for stabilization of the activity. The reaction pressure and the gas flow rate were controlled by a high-precision pressure regulator PR and a control valve CV, respectively. The reactor outlet gas was depressurized to an atmospheric pressure with CV, sampled with an automated sampling valve S, and led to an on-line connected gas chromatograph GC. Condensation of products was avoided through warming the line R-GC.

Commercial Cu–Zn-based catalyst pellets were powdered to 420–840 μm. The catalyst was reduced at 140°C under an atmospheric pressure in a flow stream of N_2 (85%) and the gas in AC2 (15%) with a space velocity of 800 h^{-1}, and exposed to 240°C for 4 h. The reduced catalyst powder (0.3 ml) was introduced to the reactor. A steady-state activity of the catalyst was obtained through methanol synthesis for 40 h with the gas in AC2 under the following conditions: pressure, 70 kg/cm^2 (1 kg/cm^2 = 98.1 kPa); temperature, 360°C; and space velocity (SV) 20,000 h^{-1} (SV = F/V; F, gas flow rate at the reactor entrance (ml/h, 0°C, 1 atm); V, catalyst volume (ml)).

The experimental conditions are summarized in Table 1. They are selected so as to include the actual conditions: temperatures are 210–300°C; pressures are 40–95 kg/cm^2; the mole ratios of the feed gas are 2.5–720 (H_2/CO), 4.3–120 (H_2/CO_2), and 0.05–180

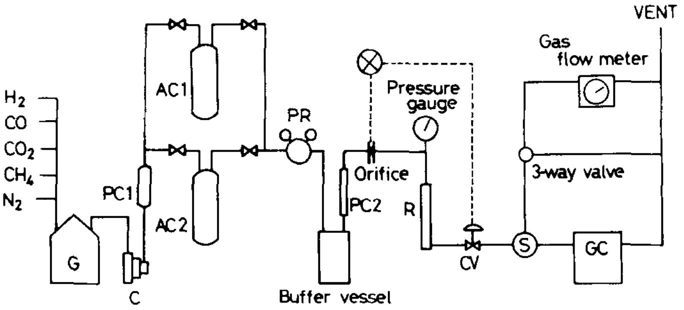

FIG. 1. Flow diagram of the apparatus for reaction rate measurements. G, gas holder; C, compressor; PC1, PC2, purifying column; AC1, AC2, accumulator; PR, pressure regulator; R, reactor; CV, control valve; S, automated sampling valve; GC, gas chromatograph.

TABLE 1

Experimental Conditions for Reaction Rate Measurements

Run No.	Pressure (kg/cm^2)	Feed gas composition (mole%)					Temperature (°C)	Space velocity ($\times 10^4$ h^{-1})
		N_2	CO	CH_4	CO_2	H_2		
K-01	95	0.54	14.70	1.85	0.73	82.03	215–300	3.3–10.5
K-02	50	0.08	26.47	0.45	1.27	71.73	215–300	1.9– 7.5
K-03	70	0.08	26.47	0.45	1.27	71.73	215–300	2.0– 9.8
K-04	95	0.08	26.47	0.45	1.27	71.73	240–290	3.5– 7.5
K-05	50	0.23	9.22	2.30	0.73	87.52	215–290	1.8– 9.4
K-06	70	0.23	9.22	2.30	0.73	87.52	215–300	2.5–13.5
K-07	95	0.23	9.22	2.30	0.73	87.52	215–300	1.8–15.0
K-08	70	0.32	18.75	32.32	0.91	47.70	215–290	4.0– 9.1
K-09	50	0.32	18.75	32.32	0.91	47.70	215–295	1.7– 6.8
K-10	60	0.78	0.15	0.70	18.80	79.57	215–290	2.0– 9.5
K-11	40	0.70	0.11	0.70	19.12	79.37	215–290	1.8– 6.5
K-12	90	0.38	0.30	34.92	9.59	54.86	215–290	3.0–15.0
K-13	50	0.41	0.31	35.02	9.55	54.71	215–290	2.3– 8.4
K-14	80	0.36	0.27	34.08	12.33	52.96	215–290	2.7–12.7
K-15	80	0.26	0.30	0.04	6.64	92.76	215–290	3.6–11.0
K-16	70	0.38	2.65	0.50	10.67	85.80	215–290	3.1–12.1
K-17	50	0.38	2.82	0.52	10.80	85.48	215–290	1.8– 8.3
K-18	70	1.90	9.63	1.29	5.06	82.12	215–290	2.6– 9.3
K-19	70	1.18	5.82	0.31	6.71	85.98	215–290	2.5– 9.8
K-20	95	0.31	7.51	0.79	1.89	89.50	215–300	3.6–15.3
K-21	70	0.31	7.51	0.79	1.89	89.50	215–300	2.6–12.1
K-22	50	0.31	7.51	0.79	1.89	89.50	215–300	2.6– 8.9
K-23	70	1.65	22.27	0.20	7.26	68.62	215–270	2.0
K-24	70	0.78	20.68	0.18	6.43	71.93	215–290	5.0

(CO_2/CO); and SV values are 17,000–160,000 h^{-1}. The measurements are divided into 24 runs, referred to either the feed gas composition or the reaction pressure. For the respective runs, the measurements were carried out at several temperatures and several gas flow rates. The outlet gas was analyzed with GC. At the end of a run, it was confirmed that the catalytic activity was unchanged, through the reproducibility of the first results.

According to the feed gas compositions, all the reaction rate measurements are classified into three subgroups: (1) CO–H_2 (K-01–K-09), (2) CO_2–H_2 (K-10–K-17), and (3) CO–CO_2–H_2 (K-18–K-24).

Additionally, it was confirmed experimentally that the rates for methanol synthesis are independent of the catalyst particle size; that is, diffusion through pores is not rate limiting. By-products were not detected.

RESULTS AND DISCUSSION

Equilibrium Process

Along with the reaction rate measurements, the equilibrium constants of [R-1] and [R-2] were measured at sufficiently low space velocities. The obtained values for both reactions are in good agreement with the calculated ones based on Ref. (*16*). The observed values are used for the equilibrium constants in the present study. Fugacity coefficients are calculated according to Berthelot's equations.[1]

---

[1] Berthelot's equations were modified a little in order to achieve better fitting of published fugacity or P–V–T data. The data include those for CH_3OH (*17, 18*), H_2O (*19, 20*), H_2 (*21*), CO (*22*), and CO_2 (*23*) under conditions similar to those employed in the present study.

The following parameters are studied for subgroup (3) ($CO-CO_2-H_2$), in detail.

$$\begin{aligned} K_{f1}^{*} &= f_{CH_3OH}/f_{CO}f_{H_2}^{2} \\ K_{f2}^{*} &= f_{CO}f_{H_2O}/f_{CO_2}f_{H_2} \qquad [1] \\ K_{f3}^{*} &= f_{CH_3OH}f_{H_2O}/f_{CO_2}f_{H_2}^{3}, \end{aligned}$$

where f_j is the fugacity of component j.

They are equilibrium constants in the equilibrium state, but in this study, the 1/SV dependence of the parameters are measured in preequilibrium states. Figure 2 shows the 1/SV dependence of K_{f2}^{*} (K-19). As shown in Fig. 2, K_{f2}^{*} shows a strange behavior. As 1/SV becomes larger, K_{f2}^{*} grows, exceeds the equilibrium value of [R-2], and nears the value again gradually from the upper side. The values of K_{f1}^{*} and K_{f3}^{*} were far less than the equilibrium ones over the whole range of 1/SV shown in Fig. 2. In conclusion, this means that it is difficult to explain the result on the assumption that only the two reactions [R-1] and [R-2] contribute to the methanol production, as follows.

Suppose that a system consists of only the two reactions [R-1] and [R-2]. Then K_{f2}^{*} increases gradually from zero with the progress of the reactions. If K_{f2}^{*} showed such a behavior in Fig. 2, it should experience the equilibrium point of (R-2) twice. Now, assume that K_{f2}^{*} has just exceeded the first equilibrium point from the lower side,

$$K_{f2}^{*\circ} = K_\gamma K_X^\circ = K_\gamma(X_{CO}^\circ X_{H_2O}^\circ/X_{CO_2}^\circ X_{H_2}^\circ), \qquad [2]$$

where K_γ is the fugacity coefficient term and X_j° is the mole fraction of component j at such a point, and that the reactions proceed a little more.

$$\begin{aligned} \text{Then, } X_{H_2}^\circ &\rightarrow X'_{H_2} = X_{H_2}^\circ - 2A + B \\ X_{CO}^\circ &\rightarrow X'_{CO} = X_{CO}^\circ - A + B \\ X_{CO_2}^\circ &\rightarrow X'_{CO_2} = X_{CO_2}^\circ + B \\ X_{CH_3OH}^\circ &\rightarrow X'_{CH_3OH} = X_{CH_3OH}^\circ + A \\ X_{H_2O}^\circ &\rightarrow X'_{H_2O} = X_{H_2O}^\circ - B \\ K_{f2}^{*\circ} &\rightarrow K_{f2}^{*\prime} = K_\gamma K'_X = K_\gamma \\ &\qquad (X'_{CO}X'_{H_2O}/X'_{CO_2}X'_{H_2}), \end{aligned}$$

where A is the change of mole fraction of CH_3OH in the reaction progress ($A > 0$) and B is the change of mole fraction of CO_2 in the reaction progress ($B > 0$). Under the present experimental conditions, it can be easily shown as below that $\Delta K_X = K_X^\circ - K'_X$ is always positive.

$$\begin{aligned} \Delta K_X &= J/(X_{CO_2}^\circ X_{H_2}^\circ X'_{CO_2} X'_{H_2}) \\ J &= B \cdot X_{CO_2}^\circ X_{H_2}^\circ (X'_{CO} + X'_{H_2O}) \\ &\quad + B \cdot X_{CO}^\circ X_{H_2}^\circ O X'_{H_2} \\ &\quad + B \cdot X_{CO_2}^\circ (B \cdot X_{H_2}^\circ + X_{CO}^\circ X_{H_2O}^\circ) \\ &\quad + A \cdot X_{CO_2}^\circ X_{H_2O}^\circ (X_{H_2}^\circ - 2X_{CO}^\circ). \end{aligned}$$

The terms of J except the last one are positive. Next, the authors show that ($X_{H_2}^\circ - 2X_{CO}^\circ$) in the last term is always positive in the feed gas systems used in the present study. The mole fraction of component j in the feed gas is denoted by X_j^{*}. The feed gas compositions in Table 1 show $X_{H_2}^{*} > 2X_{CO}^{*} + 3X_{CO_2}^{*}$ in all runs. This means that the feed gases include stoichiometrically excess H_2. Now, assume that m moles of CH_3OH are produced and n moles of CO_2 are consumed from 1 mole of the feed gas and resulting mole fractions of H_2 and CO are $X_{H_2}^\circ$ and X_{CO}°, respectively. All m, n, and $1 - 2m$ (resulting total mole number) are positive.

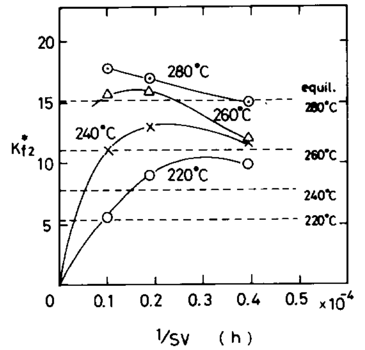

FIG. 2. Dependences of $K_{f2}^{*} = f_{CO}f_{H_2O}/f_{CO_2}f_{H_2}$ on 1/SV in subgroup (3) ($CO-CO_2-H_2$). (K-19). Broken lines, values of the equilibrium constant of [R-2]

$$\begin{aligned} \text{Then, } & X^{\circ}_{H_2} - 2X^{\circ}_{CO} \\ & = (X^{*}_{H_2} - 2X^{*}_{CO} - 3n)/(1 - 2m) \\ & > (X^{*}_{H_2} - 2SX^{*}_{CO} - 3X^{*}_{CO_2})/(1 - 2m) \\ & \qquad (\because n < X^{*}_{CO_2}) > 0. \end{aligned}$$

Accordingly, K'_X is always smaller than K°_X *in the present study. That is, whenever* K^{*}_{f2} exceeds the equilibrium point of [R-2], it always becomes smaller and no longer goes far. Therefore, the assumption that only the two reactions [R-1] and [R-2] contribute to the methanol synthesis does not agree with the result in Fig. 2. Another contribution is necessary and the addition of [R-3] makes it possible to explain the result in Fig. 2.

Villa *et al.* (*2*) carried out a kinetic study of methanol synthesis over a Cu–Zn–Al_2O_3 catalyst under conditions similar to those industrially employed, but did not report the anomaly in Fig. 2. Probably, this is due to the larger values of 1/SV employed in their study (>0.4 × 10^{-4} h).

Reaction Selectivity

Figure 3 shows the dependence of CO selectivities (Eq. [3]) and CH_3OH selectivities (Eq. [4]) on CO_2 conversions in the subgroup (2) (CO_2–H_2):

CO selectivity

$$= \frac{\text{produced CO (mole)}}{\text{consumed } CO_2 \text{ (mole)}} \times 100 \qquad [3]$$

CH_3OH selectivity

$$= \frac{\text{produced } CH_3OH \text{ (mole)}}{\text{consumed } CO_2 \text{ (mole)}} \times 100 \qquad [4]$$

In Fig. 3, CH_3OH selectivities are superior to CO selectivities in the whole range and the former is likely to be larger with a decrease in CO_2 conversions. If methanol was produced only via CO, in the region of low CO_2 conversions CH_3OH selectivities should be low, and they should approach zero as CO_2 conversions approached zero. Figure 3 does not show such a tendency but suggests that methanol is produced directly from CO_2 through [R-3].

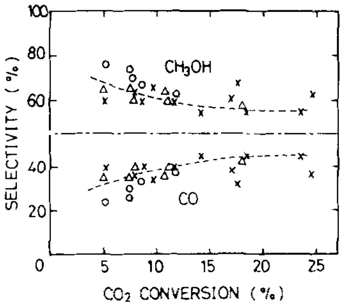

FIG. 3. Dependences of CH_3OH selectivities and CO selectivities on CO_2 conversions in subgroup (2) (CO_2–H_2). 220–240°C. (○) K-10, (△) K-12, (×) K-14.

Therefore, the evidence shown in Figs. 2 and 3 leads to the conclusion that the reaction [R-3] must be taken into account in addition to [R-1] and [R-2] in methanol synthesis from CO, CO_2, and H_2.

Kinetic Study

It is sufficient to take into account both reactions [R-1] and [R-2] in material balance. The progress of [R-1] changes total mole number. Therefore, the production rates of the respective components must be estimated from experimental data as follows,

$$\begin{aligned} r_{CH_3OH} &= d\{x/\mathrm{Cs}(1 + 2x)\}/d(1/\mathrm{SV}) \\ &= d\{-1/(2\mathrm{Cs}(1 + 2x))\}/d(1/\mathrm{SV}) \\ &\equiv dF(x)/d(1/\mathrm{SV}) \qquad [5] \\ r_{CO_2} &= d\{y/\mathrm{Cs}(1 + 2x)\}/d(1/\mathrm{SV}) \\ &\equiv -dG(x, y)/d(1/\mathrm{SV}) \qquad [6] \\ r_{CO} &= d\{z/\mathrm{Cs}(1 + 2x)\}/d(1/\mathrm{SV}) \\ &\equiv dH(x, z)/d(1/\mathrm{SV}), \qquad [7] \end{aligned}$$

where r_j is the production rate of component j (mole/liter/h); x, y, z are the mole fraction of CH_3OH, CO_2, CO, respectively; and Cs is a constant (= 22.4).

The sample results are shown in Fig. 4 (K-12), which shows the relation between the compositions of the reactor-outlet gas and the reaction temperatures. The values of $F(x)$, $G(x, y)$, and $H(x, z)$ at several temperatures are derived in Eqs. [5], [6], and [7] on the basis of the results in Fig. 4, and plotted against 1/SV values in Figs. 5a, 5b, and 5c, respectively. The slopes of the tan-

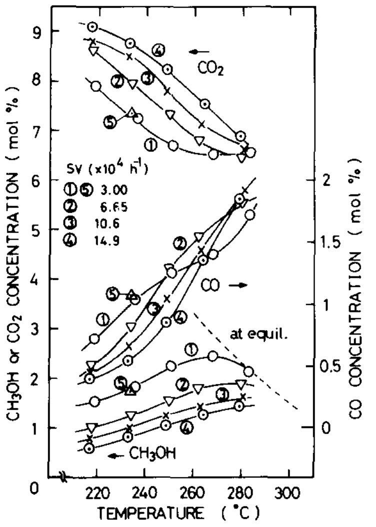

FIG. 4. Example results of reaction rate measurements (K-12). The order of measurements is 1 → 2 → 3 → 4 → 5.

gents of the respective curves in Fig. 5 correspond to the production rates of the respective components.

In the present study, rate equations in the form of a power-rate law are used for evaluation of the respective reaction's contribution.

Methanol synthesis from CO and H_2. The experiments in subgroup (1) (CO–H_2) were carried out with the feed gases of the CO_2/CO ratios less than 0.08, where the reactions of CO_2 were negligible. Equation [8] is assumed as a rate equation of CH_3OH production from CO and H_2 in subgroup (1). Equation [9] is derived from Eqs. [5] and [8];

$$r_{CH_3OH} = k_1(f_{CO}f_{H_2}^{\alpha_1})^{\alpha_2} \cdot \{1 - (f_{CH_3OH}/K_{f1}f_{CO}f_{H_2}^2)^{\beta}\} \quad [8]$$

$$k_1 \cdot Cs \cdot (1/SV) = \int 1/[(1+2x)(f_{CO}f_{H_2}^{\alpha_1})^{\alpha_2} \cdot \{1 - (f_{CH_3OH}/K_{f1}f_{CO}f_{H_2}^2)^{\beta}\}]\, dx \equiv I(x), \quad [9]$$

where $k_1 = A_1 \cdot \exp(-E_{a1}/RT)$ is the rate constant of [R-1]. $I(x)$ can be numerically solved for arbitrary values of α_1, α_2, β, and x. The values of $I(x)$ calculated from the results in subgroup (1) according to Runge–Kutta–Gill method are plotted against 1/SV. Equation [9] shows that when parameters α_1, α_2, and β are reasonable, the plotted line is regarded as the straight line passing through the origin with a slope of k_1Cs at each temperature, independent of both re-

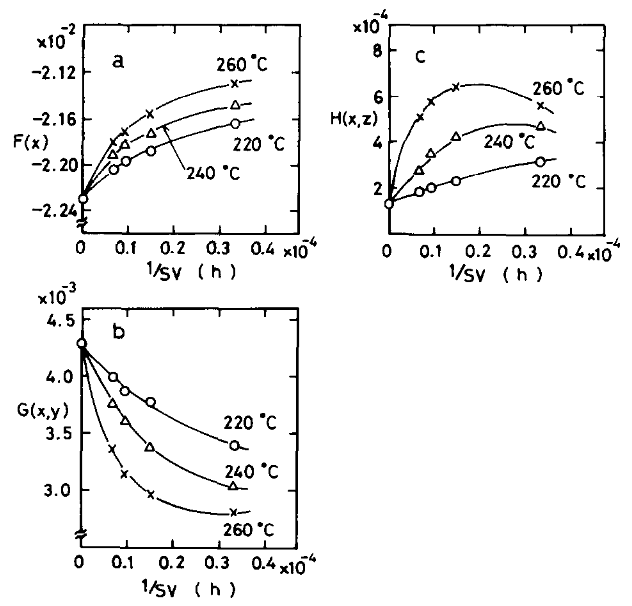

FIG. 5. 1/SV dependences of $F(x)$, $G(x, y)$, and $H(x, z)$ (K-12).

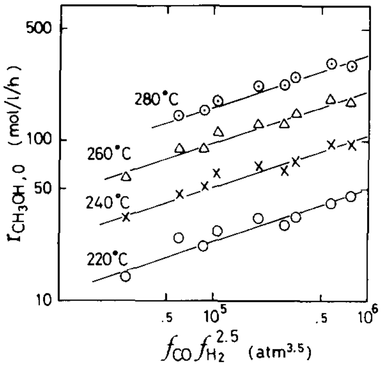

FIG. 6. Relation between the observed initial rates of CH_3OH production and $f_{CO}f_{H_2}^{2.5}$ in subgroup (1) ($CO-H_2$).

action pressures and feed gas compositions. In the present study, α_1 and α_2 are derived from the initial rates analysis (their dependences on $f_{CO}f_{H_2}^{\alpha_1}$, cf. Fig. 6), and β is adjusted to give such straight lines at the respective temperatures. In conclusion, α_1, α_2, and β are 2.5, 0.35, and 0.8, respectively. Figure 7 shows the simulation of Eq. [9] based on the values set.

The values of k_1 are evaluated from the slopes of the straight lines in Fig. 7, $k_1 = 1.03 \times 10^7 \cdot \exp(-16.6 \times 10^3/RT)$.

The CO_2/CO ratios in the feed gases in subgroup (1) are between 0.047 and 0.08. Klier *et al.* (*9*) reported that a significant increase in methanol production is observed when the CO_2/CO ratio in the feed gas is raised from zero to 0.07. In the present study such an increase is not observed, and it is supposed that the activation occurs between a CO_2/CO ratio of 0 and 0.047.

Methanol synthesis from CO, CO_2, and H_2. The initial rate values of CH_3OH production obtained in subgroup (2) (CO_2-H_2) are listed in Table 2 with those from CO and H_2 calculated by Eq. [8]. The observed values are much larger than the calculated ones. Reasonably it is attributable to the contribution of [R-3] because of the results shown in Figs. 2 and 3.

The rates of component reactions [R-1]–[R-3] are correlated with the production rates of CH_3OH, CO_2, and CO as

$$\begin{aligned} r_{CH_3OH} &= r_1 + r_3 \\ -r_{CO_2} &= r_2 + r_3 \qquad [10] \\ r_{CO} &= -r_1 + r_3, \end{aligned}$$

where r_i is the rate of [R-i] (i = 1, 2, 3).

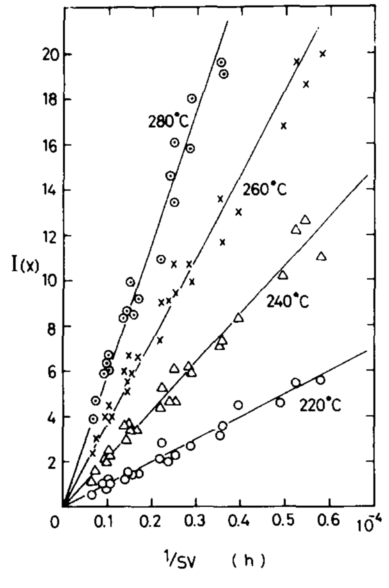

FIG. 7. Relation between $I(x)$ and 1/SV; $\alpha_1 = 2.5$, $\alpha_2 = 0.35$, and $\beta = 0.8$.

TABLE 2

Initial Rates of CH_3OH Production in Subgroup (2) (CO_2-H_2): Comparison of Observed Rates with Those from Co and H_2 Calculated by Eq. [8][a]

Run No.	Temperature (°C)	Initial rate of CH_3OH production	
		Observed	Calculated (from CO and H_2)
K-10	220	62.1	5.9
	240	108	11.5
	260	180	21.1
K-12	220	43.1	9.0
	240	77.8	17.5
	260	160	32.2
K-14	220	52.2	7.3
	240	75.6	14.1
	260	142	25.9
K-16	220	51.0	21.0
	240	106	40.5
	260	166	74.5

[a] Units are moles per liter per hour.

The initial rates of [R-2] and [R-3] in subgroup (2) are estimated with Eq. [8] and correlation [10]. Their dependences on fugacity are shown in Fig. 8. Figure 8a suggests that the initial rate of [R-2] is of first order in the fugacity of H_2, independent of that of CO_2. Figure 8b suggests that the initial rate of [R-3] is of first order in the fugacity of CO_2, independent of that of H_2. The result in Fig. 8a is different from that reported by Van Herwijnen *et al.* (*15*). Probably this is due to the differences in reaction conditions: they carried out the experiments under low pressures (1–6 atm) without the formation of methanol. In Fig. 8, the rates obtained in K-16 and K-17, which were carried out with the feed gases of about 10 times as much CO concentrations as others, fall on the same lines. This suggests that CO does not retard [R-2] in the absence of water, and it is inert in [R-3].

TABLE 3

Initial Rates of CH_3OH Production in Subgroup (3) (CO–CO_2–H_2): Comparison of Observed Rates with Calculated Ones of [R-1] and [R-3][a]

Run No.	Temperature (°C)	Initial rate of CH_3OH production		
		Observed	Calculated	
			[R-1]	[R-3]
K-18	220	32.3	31.7	14.2
	240	68.9	61.3	25.2
	260	148	113	42.8
K-19	220	33.7	27.7	18.8
	240	78.0	53.5	33.4
	260	148.3	98.4	56.8
K-20	220	42.7	45.9	7.1
	240	90.4	88.6	12.6
	260	163	163	21.4

[a] The calculated values of [R-1] were estimated by Eq. [8] and those of [R-3] were obtained on the basis of the result in Fig. 8b. Units are in moles per liter per hour.

The initial rate values of CH_3OH production obtained in subgroup (3) (CO–CO_2–H_2) are listed in Table 3, with the calculated ones of [R-1] and [R-3]. The values for [R-1] are calculated by Eq. [8] and those for [R-3] are obtained according to the results shown in Fig. 8b. Table 3 shows that the observed initial rates are smaller than the sum of the calculated ones. It has been already shown in the present study that [R-3] occurs in subgroup (3) (Fig. 2) and CO does not retard [R-3] (Fig. 8b). Then the result in Table 3 leads to the explanation that the addition of CO_2 to the feed gas lowers the initial rate of [R-1]. This seems to coincide with Klier's conclusion that at high concentrations CO_2 acts as a retardant of methanol synthesis and that it adsorbs on the active center more strongly than CO (*9*).

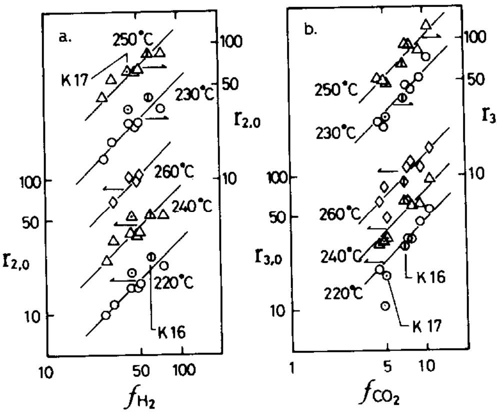

FIG. 8. Fugacity dependences of the observed initial rates of [R-2] and [R-3] in subgroup (2) (CO_2–H_2). (⦶, ⍋, ⟠) K-16, (⊙, ◬, ⟐) K-17.

When CO_2 is added to the feed gas, water is produced through [R-2] and [R-3]. Vedge *et al.* (*24*) reported that at high concentrations water retards methanol synthesis more than CO_2 (*24*). Liu *et al.* (*10*) also reported that the initial rate of methanol formation is greatly suppressed with addition of water (*10*). Therefore, water is assumed to retard methanol synthesis as well as CO_2. Additionally, through the simulation carried out with addition of the contribution of the reverse reactions of [R-2] and [R-3] and with Eq. [8], it is suggested that methanol synthesis is retarded by reaction products in the degree greater than the contribution of the reverse reactions.

On the basis of above considerations, Eqs. [11], [12], and [13] are assumed for the rate equations of [R-1], [R-2], and [R-3], respectively,

$$r_1 = k_1(f_{CO}f_{H_2}^{\alpha_1})^{\alpha_2} \cdot \{1 - (f_{CH_3OH}/K_{f1}f_{CO}f_{H_2}^2)^{\beta}\}/(1 + K_{CO_2}f_{CO_2} + K_{H_2O}f_{H_2O}) \quad [11]$$

$$r_2 = k_2 f_{H_2}(1 - f_{CO}f_{H_2O}/K_{f2}f_{CO_2}f_{H_2}) \quad [12]$$

$$r_3 = k_3 f_{CO_2}(1 - f_{CH_3OH}f_{H_2O}/K_{f3}f_{CO_2}f_{H_2}^3)/(1 + K_{H_2O}f_{H_2O}), \quad [13]$$

where $k_i = A_i \cdot \exp(-E_{ai}/RT)$ is the rate constant of [R-i] (i = 1, 2, 3); $K_j = B_j \cdot \exp(Q_j/RT)$ is the adsorption equilibrium constant of component j (j = CO_2, H_2O); A_i, B_j are preexponential factors; E_{ai} is the apparent activation energy of [R-i]; and Q_j is the adsorption heat of component j. Here, the slopes of the straight lines in Fig. 8 are assumed not to change with the addition of CO_2 adsorption term to Eq. [8], because in subgroup (2), both the contribution of [R-1] to the initial rates of [R-2] and [R-3] and the change of the initial rates of [R-1] due to the CO_2 retardation are regarded small.

The parameters k_1, α_1, α_2, and β must be the same as those previously determined; then, four parameters, k_2, k_3, K_{CO_2}, and K_{H_2O} are left for determination. From the initial rate analysis the former three were roughly estimated, and finally these four parameters are determined with all data according to Simplex method (*25*) so as to minimize the value of S defined by Eq. [14], the sum of squares of the relative deviations between observed concentration ($X_{j,0}$) and the corresponding calculated one ($X_{j,c}$).

$$S = \Sigma[\{(X_{CO,0} - X_{CO,c})/X_{CO,0}\}^2 + \{(X_{CO_2,0} - X_{CO_2,c})/X_{CO_2,0}\}^2 + 2\{(X_{CH_3OH,0} - X_{CH_3OH,c})/X_{CH_3OH,0}\}^2]. \quad [14]$$

The calculated concentrations are obtained through solving the differential equations based on material balance and reaction rates in an ordinary manner according to the Runge–Kutta–Gill method. The weight for CH_3OH was set larger than that for CO or CO_2, because the calculated values of CH_3OH concentration were found to be the most sensitive to a change of the parameter values. Consequently the parameter estimates listed in Table 4 are obtained. The goodness of fit is shown in Fig. 9, where the calculated concentrations are plotted against the observed ones for CH_3OH (Fig. 9a), CO (Fig. 9b), and CO_2 (Fig. 9c); one-fifth of the experimental data is randomly selected. Therefore, it is concluded that the reaction rates for methanol synthesis from CO, CO_2, and H_2 can be expressed by Eqs. [11]–[13].

TABLE 4

The Parameter Estimates in Eqs. [11]–[13]

$\alpha_1 = 2.5$, $\alpha_2 = 0.35$, $\beta = 0.8$

$k_1 = 1.03 \times 10^7 \cdot \exp(-16.6 \times 10^3/RT)$

$k_2 = 1.25 \times 10^{12} \cdot \exp(-28.8 \times 10^3/RT)$

$k_3 = 2.33 \times 10^7 \cdot \exp(-15.0 \times 10^3/RT)$

$K_{CO_2} = 1.86 \times 10^{-9} \cdot \exp(18.1 \times 10^3/RT)$

$K_{H_2} = 1.06 \times 10^{-7} \cdot \exp(16.7 \times 10^3/RT)$

Let us consider the methanol synthesis under the following conditions: pressure, 75 atm; temperatures, 220–260°C; space velocity, $1.0 \times 10^4\ h^{-1}$; and feed gas composition, 70% H_2 and 30% CO + CO_2. Klier *et al.* (*9*) carried out a kinetic study under the same conditions but with a space velocity of 6100 liters/kg cat./h (*9*). Figures 10 and 11 show the dependences of the methanol concentrations and the initial rates of CH_3OH production estimated by Eqs. [11]–[13], respectively, on the CO_2 concentrations in the feed gas. The experiments in the present study were carried out with the feed gases of the CO_2/CO ratios larger than 0.047; then, out of this range the estimated values are illustrated in dotted lines. The broken lines in Fig. 10 show the equilibrium concentrations, which decrease with an increase in the CO_2/CO ratio in the feed gas. The broken lines in Fig. 11 show the estimated initial rates of [R-1] and [R-3] (220°C).

Figure 10 shows that the estimated methanol concentration decreases with an increase in the CO_2/CO ratio. Figure 10 does not suggest the promoting effect of CO_2, which may appear in the range of the CO_2/

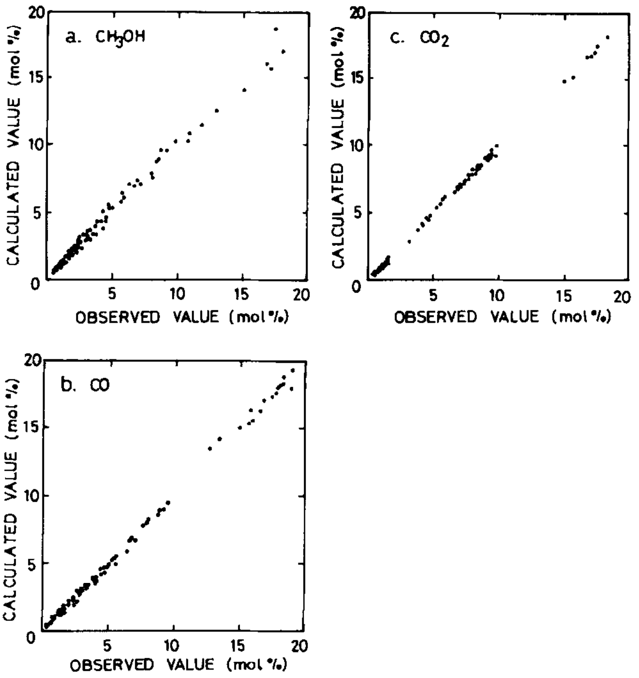

FIG. 9. Relation between the concentrations estimated by Eqs. [11]–[13] and the observed ones; one-fifth of the experimental data is randomly selected.

CO ratio less than 0.047; however, except in such regions the result in Fig. 10 is in accordance with that reported by Klier *et al.* (*9*). Figure 11 shows that the estimated

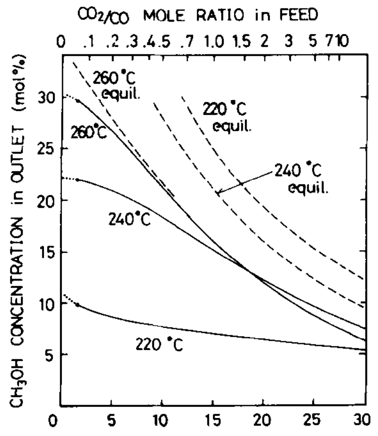

FIG. 10. Effect of CO_2 concentrations in the feed gas on the CH_3OH concentrations estimated by Eqs. [11]–[13] under the following conditions: pressure, 75 atm; SV, 10,000 h^{-1}; and the feed gas, 70% H_2 + 30% (CO + CO_2). Broken lines, values at equilibrium. Dotted lines, extrapolation.

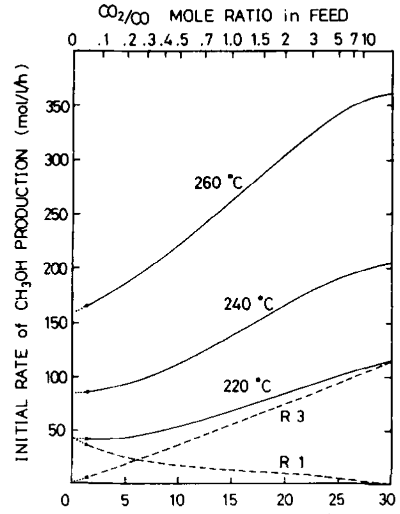

FIG. 11. Effect of CO_2 concentrations in the feed gas on the initial rates of CH_3OH production estimated by Eqs. [11]–[13] under the following conditions; pressure, 75 atm; SV, 10,000 h^{-1}; and the feed gas, 70% H_2 + 30% (CO + CO_2). Broken lines, values of [R-1] or [R-3] at 220°C. Dotted lines, extrapolation.

initial rate of CH_3OH production increases monotonously with an increase in the CO_2/CO ratio. This coincides with the result reported by Liu *et al.* (*10*). Therefore, Eqs. [11]–[13] can well explain the results of both Klier's (*9*) and Liu (*10*), which at first glance conflict with one another.

From the viewpoint of reaction rates, Eqs. [11]–[13] clarify the effect of CO_2 on the actual methanol synthesis from CO, CO_2, and H_2 as follows, though they cannot suggest its promoting effect in the lower CO_2/CO range. In the early stage of the reactions, the rate of CH_3OH production becomes larger with an increase in the CO_2/CO ratio due to the increasing contribution of [R-3]. While the reactions proceed, the amount of produced water and the influence of the equilibrium increase with an increase in the CO_2/CO ratio. As a result, under the above conditions, the amount of produced methanol decreases with an increase in the CO_2/CO ratio.

CONCLUSIONS

The reaction rates for methanol synthesis from CO, CO_2, and H_2 were measured over a Cu–Zn-based catalyst under a wide range of reaction conditions. It was concluded that three reactions [R-1], [R-2], and [R-3] take place in the synthesis. Empirical rate equations of the three reactions were derived, and on the basis of reaction rates, the effect of CO_2 was clarified.

APPENDIX: NOMENCLATURE

A_i	preexponential factor of k_i (i = 1, 2, 3)
B_j	preexponential factor of K_j (j = CO_2, H_2O)
Cs	constant (= 22.4)
E_{ai}	apparent activation energy of [R-i] (i = 1, 2, 3) (kcal/mole)
$F(x)$	function defined by Eq. [5]
$G(x, y)$	function defined by Eq. [6]
$H(x, z)$	function defined by Eq. [7]
$I(x)$	function defined by Eq. [9]
K_j	adsorption equilibrium constant of component j (j = CO_2, H_2O)
K_{fi}	equilibrium constant of [R-i] (i = 1, 2, 3)
K_{fi}^*	function defined by Eq. [1] (i = 1, 2, 3)
Q_j	adsorption heat of component j (j = CO_2, H_2O) (kcal/mole)
X_j°, X_j', X_j^*	mole fraction of component j
f_j	fugacity of component j (atm)
k_i	rate constant of [R-i] (i = 1, 2, 3)
r_i	reaction rate of [R-i] (i = 1, 2, 3) (mole/liter/h)
r_j	production rate of component j (mole/liter/h)
x, y, z	mole fraction of CH_3OH, CO_2, CO, respectively
α_1, α_2, β	exponent in rate equation

REFERENCES

1. Shah, M. J., and Stillman, R. E., *Ind. Eng. Chem.* **62**(12), 59 (1970).

2. Villa, P., Forzatti, P., Buzzi-Ferraris, G., and Pasquon, I., *Ind. Eng. Chem. Process Des. Dev.* **24**, 12 (1985).

3. Ogino, Y., and Tani, M., *Nippon Kagakukaishi* 1878 (1975).

4. Kagan, Yu. B., Lin, G. I., Rozovskii, A. Ya., Bashkirov, A. N., Naumov, I. P., Khludenev, I. K., Kudinov, S. A., and Golovkin, Yu. I., *Kinet. Katal.* **17**, 440 (1976).

5. Rozovskii, A. Ya., Lin, G. I., Liberov, L. G., Slivinskii, E. V., Loktev, S. M., Kagan, Yu. B., and Bashkirov, A. N., *Kinet. Katal.* **18**, 691 (1977).

6. Amenomiya, Y., and Tagawa, T., "Proc. 8th Int. Congr. Catal., Berlin, 1984," pp. 2–557. Dechema, Frankfurt-am-Main, 1984.

7. Kuznetsov, V. D., Shub, F. S., and Temkin, M. I., *Kinet. Katal.* **25**, 606 (1984).

8. Shub, F. S., Kuznetsov, V. D., Ivanova, R. A., Snagovskii, Yu. S., and Temkin, M. I., *Kinet. Katal.* **25**, 614 (1984).

9. Klier, K., Chatikavanij, V., Herman, R. G., and Simmons, G. W., *J. Catal.* **74**, 343 (1982).

10. Liu, G., Willcox, D., Garland, M., and Kung, H. H., *J. Catal.* **90**, 139 (1984).

11. Natta, G., *in* "Catalysis" (P. H. Emmet, Ed.), Vol. 3, p. 349. Reinhold, New York, 1955.

12. Uchida, H., and Ogino, Y., *Bull. Chem. Soc. Japan* **31**, 45 (1958).

13. Leonov, V. E., Karabaev, M. M., Tsybina, E. N., and Petrishcheva, G. S., *Kinet. Katal.* **14,** 970 (1973).
14. Lender, Yu. V., Parfenova, L. S., and Tel'nykh, K. N., *Khim. Prom.* **49,** 654 (1973).
15. Van Herwijnen, T., and De Jong, W. A., *J. Catal.* **63,** 83 (1980).
16. Soc. Chem. Eng. Japan (Ed.), "Handbook of Chemical Engineering," 4th ed. Maruzen, Tokyo, 1978.
17. Mikhailova, S. A., Kazarnovskii, J. S., and Kazarnovskaya, D. B., *Khim. Prom.* **4,** 244 (1963).
18. Zubarev, B. N., and Bagdonas, A. V., *Teploenergetika* **14,** 79 (1967).
19. Severns, W. H., "Steam, Air, and Gas Power." Wiley, New York, 1954.
20. Kell, G. S., McLaurin, G. E., and Whalley, E., *J. Chem. Phys.* **48,** 3805 (1968).
21. Wooley, H. W., Scatt, R. B., and Brickwedde, F. G., Research Paper RP1932, Vol. 41, p. 379. 1948.
22. Connoly, J. F., *Phys. Fluids* **7,** 1023 (1963).
23. Van Huff, N. E., Houghton, G., and Coull, J., *J. Chem. Eng. Data* **8,** 336 (1963).
24. Vedge, G. A., Pitchai, R., Herman, R. G., and Klier, K., "Proc. 8th Int. Congr. Catal., Berlin, 1984," pp. 2–47. Dechema, Frankfurt-am-Main, 1984.
25. Nelder, J. A., and Mead, R., *Comput. J.* **7,** 308 (1964).